The FASEB Journal article fj.14-267104. Published online August 11, 2015.

The zebrafish miR-462/miR-731 cluster is induced under hypoxic stress *via* hypoxia-inducible factor 1α and functions in cellular adaptations

Chun-Xiao Huang,* Nan Chen,* Xin-Jie Wu,* Cui-Hong Huang,* Yan He,* Rong Tang,*,† Wei-Min Wang,*,† and Huan-Ling Wang*,†,[1]

*Key Laboratory of Freshwater Animal Breeding and Key Laboratory of Agricultural Animal Genetics, Breeding and Reproduction, Ministry of Education, College of Fishery, Huazhong Agricultural University, Wuhan, Hubei, China; and †Freshwater Aquaculture Collaborative Innovation Center of Hubei Province, Wuhan, Hubei, China

ABSTRACT **Hypoxia, a unique and essential environmental stress, evokes highly coordinated cellular responses, and hypoxia-inducible factor (HIF) 1 in the hypoxia signaling pathway, an evolutionarily conserved cellular signaling pathway, acts as a master regulator of the transcriptional response to hypoxic stress. MicroRNAs (miRNAs), a major class of posttranscriptional gene expression regulators, also play pivotal roles in orchestrating hypoxia-mediated cellular adaptations. Here, global miRNA expression profiling and quantitative real-time PCR indicated that the up-regulation of the miR-462/miR-731 cluster in zebrafish larvae is induced by hypoxia. It was further validated that miR-462 and miR-731 are up-regulated in a Hif-1α–mediated manner under hypoxia and specifically target *ddx5* and *ppm1da*, respectively. Overexpression of miR-462 and miR-731 represses cell proliferation through blocking cell cycle progress of DNA replication, and induces apoptosis. *In situ* detection revealed that the miR-462/miR-731 cluster is highly expressed in a consistent and ubiquitous manner throughout the early developmental stages. Additionally, the transcripts become restricted to the notochord, pharyngeal arch, liver, and gut regions from postfertiliztion d 3 to 5. These data highlight a previously unidentified role of the miR-462/miR-731 cluster as a crucial signaling mediator for hypoxia-mediated cellular adaptations and provide some insights into the potential function of the cluster during embryonic development.—Huang, C.-X., Chen, N., Wu, X.-J., Huang, C.-H., He, Y., Tang, R., Wang, W.-M., Wang, H.-L. The zebrafish miR-462/miR-731 cluster is induced under hypoxic stress *via* hypoxia-inducible factor 1α and functions in cellular adaptations. *FASEB J.* 29, 000–000 (2015). www.fasebj.org**

Key Words: cell survival · embryonic development · low oxygen · hypoxamir

Hypoxia, or low oxygen tension, is a unique environmental stress that not only represents the insufficient oxygen supply to cells and tissues but also occurs during a range of physiologic and pathophysiological circumstances, including development, inflammation, tissue ischemia, and tumor growth (1–3). Aerobic organisms and cells have developed complex adaptive mechanisms to maintain oxygen homeostasis and evolved physiologic and biochemical responses to survive hypoxic stress (4–6). Two well-studied O_2-sensitive signaling pathways are implicated in promoting hypoxia tolerance: signaling through mTOR (mammalian target of rapamycin) that regulates mRNA translation initiation and signaling through activation of the unfolded protein response that alleviates endoplasmic reticulum stress (3, 7). Additionally, multiple hypoxia-responsive transcription factors (TFs) such as NF-κB, AP-1 (activating protein 1), and p53 are also involved in cellular oxygen sensing and homeostasis (8). However, the evolutionarily conserved hypoxia-inducible factor (HIF) signaling pathway has been recognized as a core pathway in the cellular adaptive response to hypoxic stress (9–11). HIF-1, a sensitive hypoxia-stabilized TF, controls the cellular response to hypoxia by regulating a wide variety of downstream genes involved in glycolysis, angiogenesis, erythropoiesis, cancer metabolism, proliferation, pH regulation, and apoptosis (3, 12, 13). HIF-1 is a basic-helix-loop-helix-PAS heterodimer consisting of an oxygen-sensitive HIF-1α subunit and a constitutive HIF-1β (or ARNT) subunit. Under normoxic conditions, HIF-1α becomes hydroxylated at highly conserved prolyl residues by the prolyl hydroxylase domain family, and then the hydroxylated HIF-1α is recognized by the von Hippel–Lindau tumor suppressor protein, which recruits an E3 ubiquitin ligase complex and targets HIF-1α for proteasomal degradation (9, 14). However, under hypoxic conditions,

Abbreviations: CDK2, cyclin-dependent kinase 2; David, database for annotation, visualization, and integrated discovery; HIF, hypoxia-inducible factor; hpf, hours postfertilization; HRE, hypoxia-responsive element; hypoxamir, hypoxia-regulated miRNA; miRNA, microRNA; NC, negative control; qRT-PCR, quantitative real-time PCR; RPKM, reads per kilobases

(*continued on next page*)

[1] Correspondence: College of Fishery, Huazhong Agricultural University, No. 1 Shizishan Street, Hongshan District, Wuhan, Hu 430070, China. E-mail: hbauwhl@hotmail.com

doi: 10.1096/fj.14-267104

This article includes supplemental data. Please visit *http://www.fasebj.org* to obtain this information.

prolyl hydroxylase domain activity is diminished, resulting in the stabilization of HIF-1α protein. Consequently, the stabilized and accumulated HIF-1α subunit heterodimerizes with HIF-1β and transcriptionally activates hundreds of genes involved in hypoxia adaptation by binding the core DNA sequence (RCGTG) in the hypoxia-responsive elements (HREs) (11, 15). Meanwhile, hundreds of genes are down-regulated in response to hypoxia in a HIF-1–dependent manner without direct HIF-1–promoter binding on the promoters (16), which indicates an indirect suppression mediated by activation of transcriptional repressors (17) or microRNAs (miRNAs) (18). Furthermore, some genes are directly repressed by HIF-1 binding in response to hypoxia (19, 20).

HIFs, master transcriptional regulators for oxygen homeostasis in all metazoan species, play pivotal roles in many physiologic systems in response to hypoxia. Under hypoxic conditions, HIF-1 mediates a metabolism shift from mitochondrial oxidative phosphorylation to aerobic glycolysis by activating downstream metabolism factors, including pyruvate dehydrogenase kinase 1, lactate dehydrogenase, and pyruvate kinase M2 (21, 22). In addition, mammalian embryonic development occurs in a low-oxygen environment (23), and HIFs are known to function in tissue formation and many developmental systems, such as angiogenesis and osteogenesis (24, 25), hematopoiesis (26), and hepatogenesis (27). Moreover, hypoxia response and HIF signaling may control innate and adaptive immunity by acting on immune cells in pathologic states (28).

In addition to the canonical HIF signaling pathway, more evidence suggests that miRNAs are essential contributors to cellular adaptation to hypoxic stress (29, 30). Over the past 2 decades, miRNAs, a group of endogenous small noncoding RNAs about 22 nucleotides in length, have emerged as critical posttranscriptional regulators (31). In general, miRNAs negatively regulate gene expression by binding the 3′ UTR of specific mRNA targets with their seed region (nucleotides 2 to 8), resulting in mRNA degradation or translational repression (32–34). Also, they may act through promoter-directed transcriptional activation (35) or silencing (36). miRNAs were reported to be implicated in a wide range of physiologic and cellular processes, including angiogenesis (37), hematopoiesis (38), erythropoiesis (39), tumorigenesis (40), glycolysis (41), cell proliferation and differentiation (42), cell cycle and apoptosis (43), and DNA repair (44). miRNA genes are often clustered and can modulate a complex signaling pathway more efficiently (45). Given that miRNA transcription is primarily mediated by RNA polymerase II, the miRNA expression can also be regulated by canonical TFs such as HIF-1 (46, 47). Additionally, emerging evidence indicates that miRNA expression is also regulated by certain external stimuli (48–50), especially by hypoxic stress, an established pivotal regulator of miRNA transcription, biogenesis and function (51).

As noncoding and small molecules, miRNAs act as a flexible switch enabling rapid, effective, and reversible fine-tuning of cellular response to hypoxic stress. Recent studies have identified an expanding group of specific hypoxia-regulated miRNAs, termed hypoxamirs, and demonstrated their important roles in the cellular hypoxia-adaptive response through monitoring and adjusting targets involved in critical physiologic and cellular processes (30, 52). Multiple lines of evidence indicate that the transcription of a subset of hypoxamirs is directly induced by HIF-1, especially the master hypoxia-regulated miRNA (hypoxamir) miR-210, which is potently induced by hypoxia in a HIF-1α–dependent manner and in turn stabilizes HIF-1α through positive feedback regulation (53). In addition, miR-210 is recognized as a unique and pleiotropic hypoxamir that is evolutionarily conserved and ubiquitously expressed in hypoxic cell and tissue types (54, 55). However, most miRNAs appear to be regulated by hypoxia only in certain cellular or tissue contexts (30), and our understanding remains limited about the physiologic functions of individual hypoxamirs in zebrafish at the embryonic and cellular levels.

In the present study, we identified the hypoxia-regulated miRNAs in zebrafish and investigated the potential roles of specific hypoxamirs in cellular adaptations. We demonstrated that the teleost-specific miR-462/miR-731 cluster is hypoxia-induced in zebrafish larvae and ZF4 (zebrafish embryo fibroblast-like cell lines) cells, and the role of the cluster in regulating cell survival was further confirmed by experiments. Additionally, we characterized, for the first time, the dynamic expression and the specific distribution of miR-462/miR-731. These findings facilitate the understanding of the crucial roles of zebrafish miR-462/miR-731 cluster in cellular adaptation to hypoxic stress, as well as its potential functions during embryonic development.

MATERIALS AND METHODS

Fish husbandry and hypoxia exposure

Adult AB strain zebrafish (*Danio rerio*) were raised and maintained on a 14/10 h light–dark schedule in the recirculating water system (28 ± 1°C). Zebrafish embryos were cultured in embryo medium until postfertiliztion d 6, followed by 24 h exposure to hypoxic (dissolved oxygen, 1.0 mg/L) or normoxic (dissolved oxygen, 7.0 mg/L) conditions. Three groups ($n = 30$) of zebrafish larvae from each condition were collected for miRNA cloning and expression profiling. Embryos and larvae at different developmental stages were collected for miRNA expression analysis.

miRNA high-throughput sequencing and bioinformatics analysis

Small RNAs were isolated from the embryos exposed to hypoxia or normoxia using the mirVana miRNA Isolation Kit (Life Technologies, Carlsbad, CA, USA). RNA abundance and quality were examined using the NanoDrop 2000 (Thermo Scientific, Carlsbad, CA, USA) and Agilent 2100 Bioanalyzer (Agilent Technologies, Santa Clara, CA, USA). The small RNAs were ligated to 5′ and 3′ single-stranded adaptors and reversely transcribed to cDNA libraries. The amplified cDNA constructs

(*continued from previous page*)

per million reads; shRNA, short hairpin RNA; TF, transcription factor; ZF4, zebrafish embryo fibroblast-like cell lines

were further purified and then sequenced on an Illumina Hiseq2000 sequencer (San Diego, CA, USA) according to the manufacturer's protocol.

First, the adaptor sequences and low quality reads were filtered out to obtain the final clean reads, and the remaining sequences were mapped to reference zebrafish genome (Zv9) using Bowite software (*http://bowtie.cbcb.umd.edu*) with 1 mismatch tolerance. Next, the matched reads were annotated to miRBase 19.0, the Ensembl noncoding RNA database, and the RepBase Repeat-Masker database to identify known miRNA sequences and separate out different categories of noncoding RNA (rRNA, tRNA, small nuclear RNA, small nucleolar RNA, miscellaneous RNA) and genomic repeats. Finally, the unannotated small RNA sequences were further identified for novel miRNA genes using the prediction software miRDeep (Friedländer and Nikolaus Rajewsky Systems Biology Group, Max Delbrück Center, Berlin-Buch, Germany; *https://www.mdc-berlin.de/10663315/de/research/research_teams/systems_biology_of_gene_regulatory_elements/resources/miRDeep.tgz*) and the RNA structure analysis software RNA-fold (ViennaRNA package 2.0; Institute for Theoretical Chemistry, University of Vienna, Währingerstraße, Vienna, Austria; *http://www.tbi.univie.ac.at/RNA/, RNAfold 2.1.9*).

The expression levels of known miRNAs were computationally normalized to RPKM (reads per kilobases per million reads) by Cufflinks software (Cole Trapnell Lab, University of Washington, Seattle, WA, USA; *http://cole-trapnell-lab.github.io/cufflinks/*). The fold change and *P* value were calculated with DESeq (European Molecular Biology Laboratory, Heidelberg, Germany; *http://www-huber.embl.de/users/anders/DESeq/*) from R software, with the significantly differential expression accepted at $P \leq 0.05$ and fold change ≥ 2.0. TargetScan 6.2 (Whitehead Institute for Biomedical Research, Cambridge, MA, USA) and MicroCosm Targets (version 5; European Molecular Biology Laboratory–European Bioinformatics Institute, Hinxton, Cambridge, United Kingdom; *http://www.ebi.ac.uk/enright-srv/microcosm/htdocs/targets/v5/*) algorithms were used to predict putative mRNA targets of differentially expressed miRNAs, and then the predicted result was associated with mRNA differential expression profile in our previous study (data not shown). The gene ontology and KEGG pathway analyses were carried out by the Kobas 2.0 (Center for Bioinformatics, Peking University, Beijing, China; *http://kobas.cbi.pku.edu.cn/home.do*) and database for annotation, visualization, and integrated discovery (David; Bioinformatics Resources 6.7, National Institutes of Health, National Institute of Allergy and Infectious Diseases, Bethesda, MD, USA; *https://david.ncifcrf.gov/*) functional annotation tools. Each gene ontology term and KEGG pathway was computationally enriched, and the *P* value was calculated to estimate the statistical significance.

Quantitative real-time PCR

Total RNA containing miRNA was isolated using Trizol reagent (Invitrogen, Carlsbad, CA, USA) by following the manufacturer's instructions with slight modifications. Quantitative real-time (qRT)-PCR was performed with gene-specific primers for *ddx5, ppm1da,* and 18S rRNA (reference gene) listed in **Table 1** using Sybr Green Mix reagent (Takara, Dalian, Shandong, China). To quantify miRNA expression, qRT-PCR was performed using primers matching the desired miRNAs (Table 1) by stem-loop RT-PCR as described previously (56). The small nucleolar RNA U6 was used as the reference gene for normalization. The reactions were carried out on Rotor-Gene Q (Qiagen, Hilden, Germany).

miRNA expression analysis

Whole-mount miRNA *in situ* hybridization was performed using 3′-DIG–labeled miRcury locked nucleic acid probes (Exiqon, Vedbaek, Denmark) (Supplemental Table S1) as previously described (57, 58). The hybridization temperature used was

TABLE 1. *Primers used in qRT-PCR for miRNA expression validation*

Primer name	Primer sequence (5′–3′)
ZB-qRT-*ddx5*-F	AACGGGCACAGCCTACACA
ZB-qRT-*ddx5*-R	TAAGAGTCACCACCACTACGG
ZB-qRT-*ppm1da*-F	GGCTCTGTTTGCGGTGTT
ZB-qRT-*ppm1da*-R	AGTTGTGCCCGATGTGCT
ZB-qRT-18s rRNA-F	CGGAGGTTCGAAGACGATCA
ZB-qRT-18s rRNA-R	GGGTCGGCATCGTTTACG
RT-miR-430a	CTCAACTGGTGTCGTGGAGTCGGCAATTCAGTTGAGCTACCCCA
RT-miR-430b	CTCAACTGGTGTCGTGGAGTCGGCAATTCAGTTGAGCTACCCCA
RT-miR-430c	CTCAACTGGTGTCGTGGAGTCGGCAATTCAGTTGAGCTACCCCA
RT-miR-462	CTCAACTGGTGTCGTGGAGTCGGCAATTCAGTTGAGAGCTGCAT
RT-miR-731	CTCAACTGGTGTCGTGGAGTCGGCAATTCAGTTGAGCGATCCGG
RT-miR-459-5p	CTCAACTGGTGTCGTGGAGTCGGCAATTCAGTTGAGCAGGATGA
RT-miR-150	CTCAACTGGTGTCGTGGAGTCGGCAATTCAGTTGAGCACTGGTA
RT-miR-451	CTCAACTGGTGTCGTGGAGTCGGCAATTCAGTTGAGAACTCAGT
RT-U6	AAAACAGCAATATGGAGCGC
qRT-miR-430a-F	CGGGCGGTAAGTGCTATTTGTTGG
qRT-miR-430b-F	CGGGCGGAAAGTGCTATCAAGTT
qRT-miR-430c-F	GCGGCTAAGTGCTTCTCTTTGGG
qRT-miR-462-F	CGGGCGTAACGGAACCCATAAT
qRT-miR-731-F	GGCGGGCAATGACACGTTTTCTC
qRT-miR-459-5p-F	CGGGCGGTCAGTAACAAGGATTC
qRT-miR-150-F	CGGCGTCTCCCAATCCTTGTACC
qRT-miR-451-F	CGGGCGGAAACCGTTACCATTAC
qRT-Reverse	TCAACTGGTGTCGTGGAGTCGGC
qRT-U6-F	TGCTCGCTACGGTGGCACA
qRT-U6-R	AAAACAGCAATATGGAGCGC

51°C for miR-462 and 54°C for miR-731 locked nucleic acid probes. The signals were visualized by nitro blue tetrazolium/5-bromo-4-chloro-3-indolyl phosphate (Gen-View Scientific, Galveston, TX, USA). Embryos were mounted in glycerol and photographed with a Leica MZ7.5 stereomicroscope (Leica, Wetzlar, Germany).

Semi–qRT-PCR of miR-462/miR-731 cluster was performed using Moloney murine leukemia virus reverse transcriptase (Promega, Madison, WI, USA) and the specific primers listed in Table 1 according to the manufacturer's instructions.

Plasmid construction

The promoter fragment of the miR-462/miR-731 cluster containing a predicted HRE (HIF-1α binding motif) was amplified and subcloned into the luciferase reporter vector pGL3-Basic (Promega). The construct harboring 9 HRE motifs of the VEGF gene was used as a positive control. For overexpression of Hif-1α, the coding sequence (CDS) of zebrafish *hif-1α* was cloned and inserted into pCMV-Myc vector (Clontech Laboratories, Mountain View, CA, USA).

The wild-type or mutant 3′ UTR segments of *ddx5* and *ppm1da* containing the putative miR-462 or miR-731 target sites were amplified and inserted into the psiCHECK-2 dual-luciferase reporter vector (Promega). All the primers used are listed in **Table 2**, and all recombined plasmids were verified by sequencing.

Cell culture and hypoxia-mimicking treatment

HeLa and ZF4 cell lines (Cell Collection Center for Freshwater Organisms, Huazhong Agricultural University) were cultured in a 5% CO_2 incubator (Thermo Scientific) containing DMEM and DMEM/F12 1:1 medium (Hyclone, Carlsbad, CA, USA) supplemented with 10% fetal bovine serum at 37 and 28°C, respectively.

To simulate hypoxic condition, ZF4 cells cultured in 6-well plates were treated with 100 and 200 μM cobalt chloride ($CoCl_2$) (Sigma-Aldrich, St. Louis, MO, USA) for 0 (control), 2, 4, 6, 8, 12, and 24 h before being collected for isolation of total RNA (including miRNA) and protein. HeLa cells overexpressed with zebrafish Myc-tagged Hif-1α were stimulated with 100 μM $CoCl_2$ for 0 (control), 4, 8, 12, and 24 h before being collected for protein isolation.

Transient transfection and luciferase assays

Transient transfection was performed using Lipofectamine 2000 (Invitrogen) according to the manufacturer's protocol. For HRE activity verification, HeLa cells were seeded in 24-well plates and cotransfected with Myc-tagged Hif-1α construct or empty vector (control), the indicated pGL3 HRE-luciferase reporter, and the pRL-TK *Renilla* luciferase reporter (internal control) (Promega). The cells were then stimulated with 100 μM $CoCl_2$ for 4 h before luciferase assay. For the target detection of miR-462 and miR-731, miRNA mimics or miRNA-NC (negative control) (GenePharma, Shanghai, China) and corresponding psiCHECK-2 3′ UTR dual-luciferase reporter were cotransfected into HeLa cells. Firefly and *Renilla* luciferase activities were measured at 24 h after transfection using Dual-Luciferase Reporter Assay System (Promega) according to the manufacturer's instructions.

ZF4 cells were cultured in 6-well plates and transfected separately with miR-462 mimics, mimics-NC, miR-462 inhibitor, and inhibitor-NC (GenePharma). At 24 to 48 h after transfection, the cells were collected for total RNA (including miRNA) and protein isolation.

Western blot analysis

HeLa or ZF4 cells were lysed in RIPA buffer with 1% PMSF (ComWin Biotech, Beijing, China). Protein extracts were separated by SDS-PAGE and transferred to the PVDF membrane (EMD Millipore, Billerica, MA, USA). The membrane was blocked with 5% nonfat dry milk in Tris-buffered saline for 1 h at room temperature, followed by 2 h incubation at room temperature with specific primary antibodies against DDX5 (1:100) and CDK2 (cyclin-dependent kinase 2; 1:1000) (Aviva Systems Biology, San Diego, CA, USA), Hif-1α (1:3000) (the homemade polyclonal antibody against zebrafish Hif-1α was prepared using prokaryotic expression system, affinity-purified and generated in rabbits), β-actin (1:500) (Boster, Wuhan, Hubei, China), or C-Myc-tag (1:500) (Biodragon Immunotechnologies, Beijing, China). The protein level was detected using Odyssey CLx Infrared Imaging System (Li-Cor Biosciences, Lincoln, NE, USA) according to the manufacturer's instructions after 1 h incubation at room temperature with IRDye 800CW anti-rabbit secondary antibody (1:10,000) (Li-Cor Biosciences).

Cell proliferation assay

ZF4 cells were grown in a 96-well plate at a density of 1×10^4 cells per well and transfected separately with 50 and 100 nM miR-462 mimics, 50 and 100 nM miR-731 mimics, and miRNA-NC. Cell proliferation was determined at 12, 24, 36, 48, 60, and 72 h after transfection using the Cell Counting Kit-8 (CCK-8) (Beyotime

TABLE 2. *Primers used in plasmid construction*

Primer name	Primer sequence (5′–3′)
miR-HRE-senseP	CTCGAGTGTTGCTGGACGTGTTTTTTCAGC
miR-HRE-antisenseP	AAGCTTGTCATACCTCATACTCTTTACACTTACAT
ZB-*hif1α*-CDS-F	ACGCGTCGACAATGGATACTGGAGTTGTCACTG
ZB-*hif1α*-CDS-R	AAATATGCGGCCGCTCAGTTGACTTGGTCCAGAGC
ZB-*ddx5*-3′UTR-F	CTCGAGTGGTGGTGACTCTTACGGC
ZB-*ddx5*-3′UTR-Rm	ACATAGGTCGGGCAAGATTAAGAT
ZB-*ddx5*-3′UTR-Fm	ATCTTGCCCGACCTATGTATCTAT
ZB-*ddx5*-3′UTR-R	GCGGCCGCAAAAAAAGGAAGGGGTGG
ZB-*ppm1da*-3′UTR-F	CTCGAGAAACCAAATCCTGAAACAAG
ZB-*ppm1da*-3′UTR-Rm-1	ACCTATTGCCACAGGGTTAAGAT
ZB-*ppm1da*-3′UTR-Fm	TTAACCCTGTGGCAATAGGTTTA
ZB-*ppm1da*-3′UTR-R	GCGGCCGCAGTTTAGAATGACACTTACTCCCA
ZB-*ppm1da*-3′UTR-Rm-2	GCGGCCGCAGTTTAGACTCACTCTTACTCCCA

TABLE 3. *Known miRNAs responsive to hypoxia*

miRNA ID	Sequence count		RPKM		Fold change	*P*
	Control	Hypoxia	Control	Hypoxia		
dre-miR-181a	45,181	17,611	377,782.75	107,830.84	0.29	0.000066**
dre-miR-430a	2234	2016	18,679.68	12,343.82	0.66	0.292633
dre-miR-430b	3941	2371	31,520.10	13,886.26	0.44	0.021461*
dre-miR-430c	418	249	3495.12	1524.61	0.44	0.075833
dre-miR-150	32	140	267.57	857.21	3.20	0.034151*
dre-miR-459-5p	662	4858	5535.34	29,745.17	5.37	0.000008**
dre-miR-2190	214	1004	1711.57	5880.14	3.44	0.005400**
dre-miR-462	19	124	158.87	759.24	4.78	0.007625**
dre-miR-731	254	751	1946.85	4215.12	2.17	0.076263
dre-miR-451	329	1144	2750.95	7004.63	2.55	0.030000*

Fold change, expression fold change represented by RPKM ratio of 2 libraries (hypoxia/normoxia); $^{**}P < 0.01$. $^{*}0.01 < P < 0.05$.

Institute of Biotechnology, Haimen, Jiangsu, China) according to the manufacturer's protocol.

Cell cycle assay

After 24 h transfection separately with miR-462 mimics, miR-731 mimics, and miRNA-NC, ZF4 cells were treated with nocodazole (100 ng/ml) (Sigma), followed by an additional 12 h incubation at 28°C and overnight fixation in 70% cold ethanol at 4°C. After washing in PBS, the cells were incubated with RNase A for 30 min at 37°C and stained with propidium iodide using the Cell Cycle Detection Kit (KeyGen BioTeck, Nanjing, Jiangsu, China) before flow cytometry analysis. Corresponding cell lysates were collected for detection of Cdk2 protein level.

Apoptosis analysis

ZF4 cells were transfected separately with miR-462 mimics and miR-731 mimics and miRNA-NC. At 48 h after transfection, the cells were collected, washed twice in cold PBS, and stained with annexin V–FITC/propidium iodide for 15 min in the dark using the Apoptosis Detection Kit (KeyGen BioTeck). The apoptosis analysis was performed in triplicate by flow cytometry.

Statistical analysis

All analyses were performed in triplicate, and all data are shown as means ± SE. Statistical difference was evaluated by Student's *t* test, with $P \leq 0.05$ considered statistically significant.

RESULTS

Small RNA profiling in hypoxia-exposed zebrafish

The deep sequencing of small RNA libraries derived from zebrafish larvae subjected to normoxia and hypoxia exposure was performed. After eliminating low-quality reads and adaptor sequences, 98.28 and 95.62% clean reads from the normoxia and hypoxia groups were obtained, with the majority of them being 20 to 25 nt in size, which is typical for Dicer digestion products. Altogether, 82.95 and 91.06% clean sequences were mapped to the zebrafish genome, with the known mature miRNAs accounting for 70.02 and 71.81%, respectively. The unannotated sequences were analyzed for identification of potential novel miRNAs. A total of 129 and 212 novel miRNAs were predicted from the 2 groups, respectively, with 102 of them in common. Among these putative novel miRNAs, some of them showed a >2-fold read change under hypoxic stress (Supplemental Table S2).

Hypoxia exposure misregulates miRNA expression in zebrafish

To identify the hypoxia-regulated miRNAs in zebrafish, the expression abundance of 247 known miRNAs collected in miRBase were detected. Seven miRNAs were determined to be differentially expressed under hypoxic conditions, with 5 of them up-regulated and 2 down-regulated (**Table 3**). Information from miRBase revealed that dre-miR-462 and dre-miR-731 were clustered on chromosome 8 (within 200 bp) and showed the possibility of consistent up-regulation under hypoxic stress (Table 1). To further validate the miRNA profiling data, the expression patterns

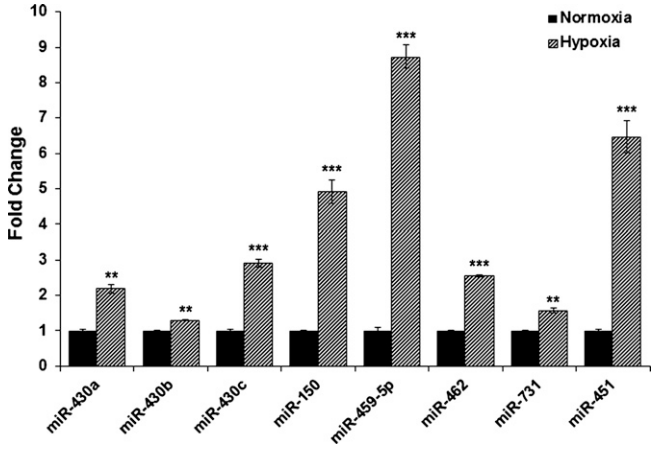

Figure 1. Expression levels of 8 miRNAs in response to hypoxic stress evaluated by qRT-PCR. U6-1 is used as endogenous control. Values represent fold change compared with normoxic control (means ± SE, $n = 3$). $^{**}P < 0.01$, $^{***}P < 0.001$, independent samples Student's *t* test.

of 8 candidate hypoxamirs including the zebrafish miR-430 family and the miR-462/miR-731 cluster were examined by qRT-PCR, indicating that all the 8 miRNAs including the miR-462/miR-731 cluster are significantly up-regulated under hypoxic stress (**Fig. 1**).

Predicted targets of differentially expressed miRNAs are involved in hypoxia-adaptive responses

A total of 2050 putative targets of these candidate hypoxamirs were predicted. The GO analysis result showed that the putative targets were mainly involved in several hypoxia-adaptive processes, such as oxidoreductase activity, endoplasmic reticulum, oxidation-reduction process, cell growth, glycolysis, unfolded protein binding, transcription regulator activity, GTPase activity, blood vessel morphogenesis, and DNA repair (Supplemental Table S3). Additionally, most of the targets were assigned to metabolism-related signaling pathways, and a number of them were also involved in other important pathways, such as nuclear receptor transcription pathway, glycolysis, methylation, and TGF-β signaling pathway (Supplemental Table S4).

Hif-1α contributes to the up-regulation of hypoxia-induced miR-462/miR-731 cluster

We investigated the involvement of Hif-1α in the up-regulation of miR-462/miR-731 cluster under hypoxia. As shown in **Fig. 2*A***, hypoxia treatment up-regulated the expression of endogenous miR-462/miR-731 cluster, whereas knockdown of Hif-1α (under normoxic condition) by short hairpin RNA (shRNA) expression vector injection down-regulated miR-462/miR-731 levels. The efficiency of shRNA was confirmed by demonstrating the decreased Hif-1α mRNA and protein levels in our previous study (unpublished data). To further investigate the transcriptional regulation of the miR-462/miR-731 cluster by Hif-1α under hypoxic conditions, we searched the 800 nt region upstream

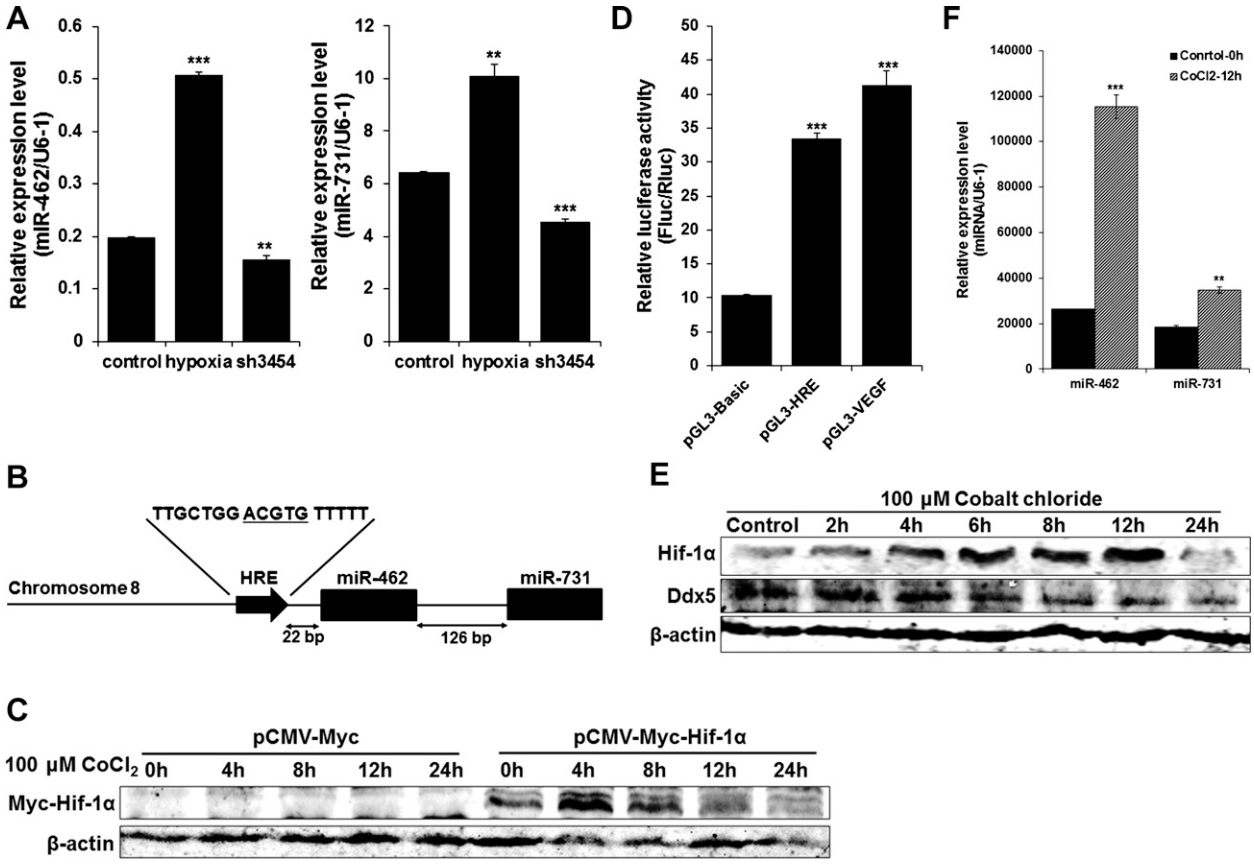

Figure 2. Hif-1α mediates hypoxia-induced up-regulation of miR-462/miR-731 cluster in zebrafish. *A*) Zebrafish embryos exposed to hypoxic condition (dissolved oxygen, 1.0 mg/L) or injected with HIF-1α shRNA expression vector (sh3454) (under normoxic condition) were collected. miR-462 and miR-731 expression was assessed by qRT-PCR. U6-1 is used as endogenous control. Values represent means ± SE ($n = 3$, $^{**}P < 0.01$, $^{***}P < 0.001$). *B*) structure of miR-462/miR-731 locus. Potential HRE motif (core sequence is underlined) was identified 22 bp upstream of miR-462/miR-731 cluster. *C*) HeLa cells transfected with pCMV-Myc-Hif-1α or pCMV-Myc empty vector (NC) was subjected to treatment of 100 μM $CoCl_2$ for 0, 4, 8, 12, and 24 h. Protein levels of zebrafish Hif-1α were detected using anti–c-Myc-tag. β-Actin is used to normalize protein levels. *D*) Luciferase reporter harboring miR-462/miR-731 HRE (pGL3-HRE) was cotransfected with pCMV-Myc-Hif-1α into HeLa cells. Luciferase activities were detected after stimulating with 100 μM $CoCl_2$ for 4 h, and firefly luciferase expression was normalized to *Renilla* luciferase. Construct pGL3-VEGF serves as positive control. Results are presented as means ± SE ($n = 3$, $^{***}P < 0.001$). *E*) Protein detection of Hif-1α and Ddx5 in ZF4 cells treated with 100 μM $CoCl_2$ for 0 to 24 h. β-Actin is used to normalize protein levels. *F*) Expression of miR-462 and miR-731 in ZF4 cells treated with 100 μM $CoCl_2$ for 12 h. Values are means ± SE ($n = 3$, $^{**}P < 0.01$, $^{***}P < 0.001$).

of the transcription start site of the cluster and identified a putative HRE motif at just the 22 nt upstream from the cluster (Fig. 2*B*). Western blot analysis indicated that zebrafish Hif-1α can be overexpressed in HeLa cells by transfection with pCMV-Myc-Hif-1α, and the expression level was significantly increased after hypoxia-mimicking treatment with $CoCl_2$ for 4 to 8 h (Fig. 2*C*). The luciferase reporter assay showed that miR-462/miR-731 HRE reporter activity was increased >3-fold by overexpression of zebrafish Hif-1α (Fig. 2*D*). In addition, to simulate a hypoxic environment, we treated ZF4 cells with $CoCl_2$ and found that the optimal condition for induction of endogenous Hif-1α was 100 μM $CoCl_2$ (Supplemental Fig. S1), under which Hif-1α was significantly up-regulated in a time-dependent manner and reached the highest level after 12 h of treatment (Fig. 2*E*), and the expression of the miR-462/miR-731 cluster was significantly induced at the same time (Fig. 2*F*).

miR-462 and miR-731 target *ddx5* and *ppm1da*, respectively

On the basis of the target prediction, DEAD (Asp-Glu-Ala-Asp) box helicase 5 (*ddx5*, p68) and protein phosphatase, $Mg2^+/Mn2^+$ dependent, 1 Da (*ppm1da*) were identified as downstream targets of miR-462 and miR-731, respectively, with complementary binding sites detected on the 3′ UTRs (**Fig. 3*A***). To evaluate the functions of miR-462 and miR-731 at target 3′ UTRs, the dual-luciferase reporter constructs carrying *ddx5* or *ppm1da* 3′ UTR (wild-type or mutant) were cotransfected with miRNA-462 mimics or miR-731 mimics, showing that luciferase activity of the wild-type construct was significantly reduced by corresponding miRNA mimics, but not that of the mutant construct (Fig. 3*B*). Furthermore, 2 effective miR-731 binding sites were identified on *ppm1da* 3′ UTR (547–554 and 673–679), with the site of 547–554 verified as the prominent one (Fig. 3*B*).

To further confirm the negative regulatory effect of miR-462 on endogenous Ddx5 protein, miR-462 overexpression and knockdown were carried out in ZF4 cells by transfection with miR-462 mimics or inhibitor. The transfection efficiency was determined by qRT-PCR (Fig. 3*C*). The Ddx5 mRNA and protein levels were significantly down-regulated by miR-462 mimics but increased by the miR-462 inhibitor (Fig. 3*D, E*). Additionally, in contrast to Hif-1α and miR-462/miR-731 cluster, the endogenous Ddx5 protein level was significantly reduced in cells treated with $CoCl_2$ in a time-dependent manner (Fig. 2*E*). These

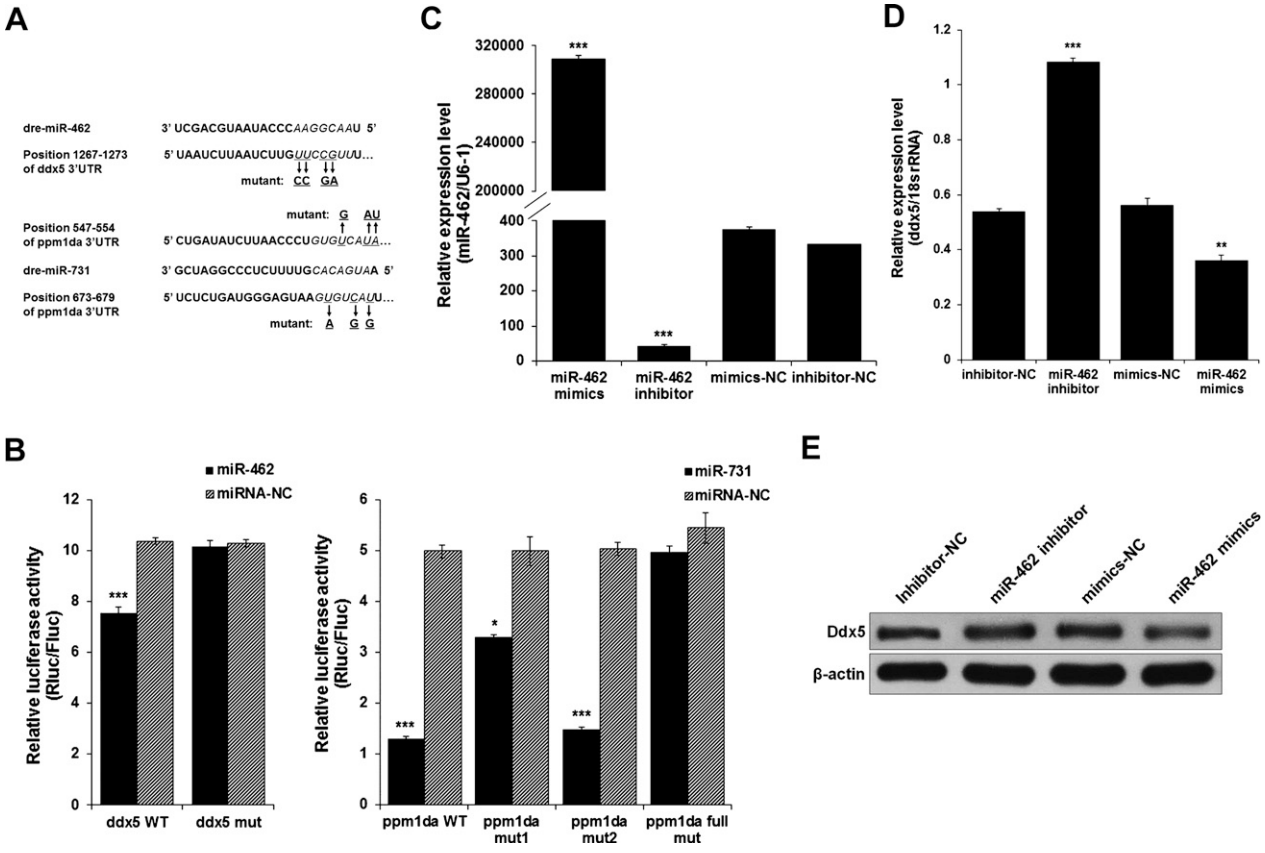

Figure 3. miR-462 and miR-731 directly target *ddx5* and *ppm1da*, respectively, by binding 3′ UTR. *A*) miRNA seed sequences and their complementary sequences on 3′ UTR are highlighted in italics. Mutant sites are indicated by arrows. *B*) miR-462 or miR-731 mimics were cotransfected with *ddx5* or *ppm1da* 3′ UTR dual-luciferase reporters into HeLa cells. *Renilla* luciferase activities were detected and normalized to firefly luciferase (internal control). Results represent means ± SE ($n = 3$, $^*P < 0.05$, $^{***}P < 0.001$). *C*) Transfection efficiency of miR-462 mimics and inhibitor was detected by qRT-PCR. All data are means ± SE ($n = 3$, $^{***}P < 0.001$). *D*) *Ddx5* mRNA expression was detected by qRT-PCR. 18S rRNA is used as endogenous control. Values represent means ± SE ($n = 3$, $^{**}P < 0.01$, $^{***}P < 0.001$). *E*) Western blot analysis of Ddx5 protein expression in ZF4 cells was performed at 48 h after overexpression or knockdown of endogenous miR-462. β-Actin is used to normalize protein levels.

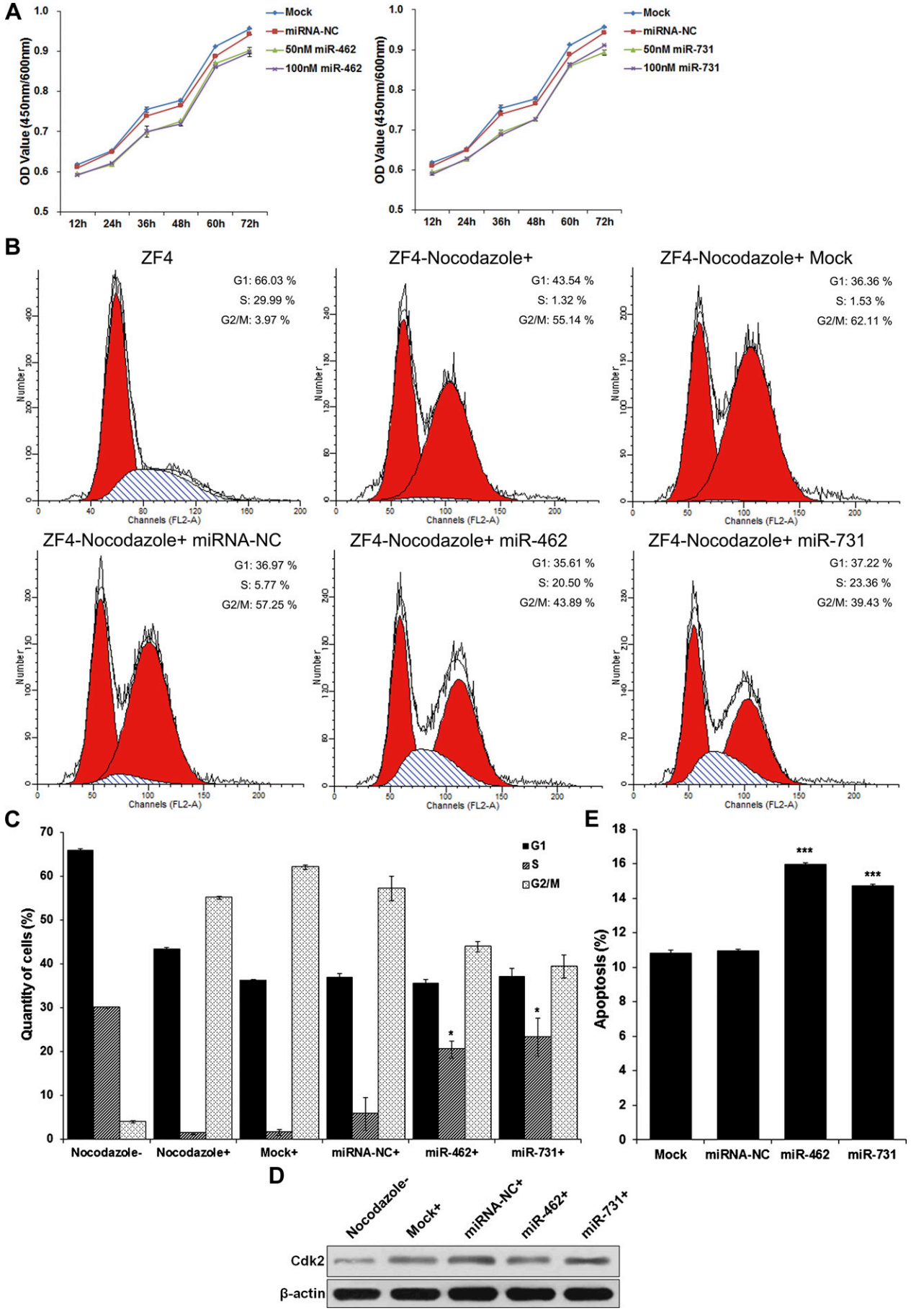

(*continued on next page*)

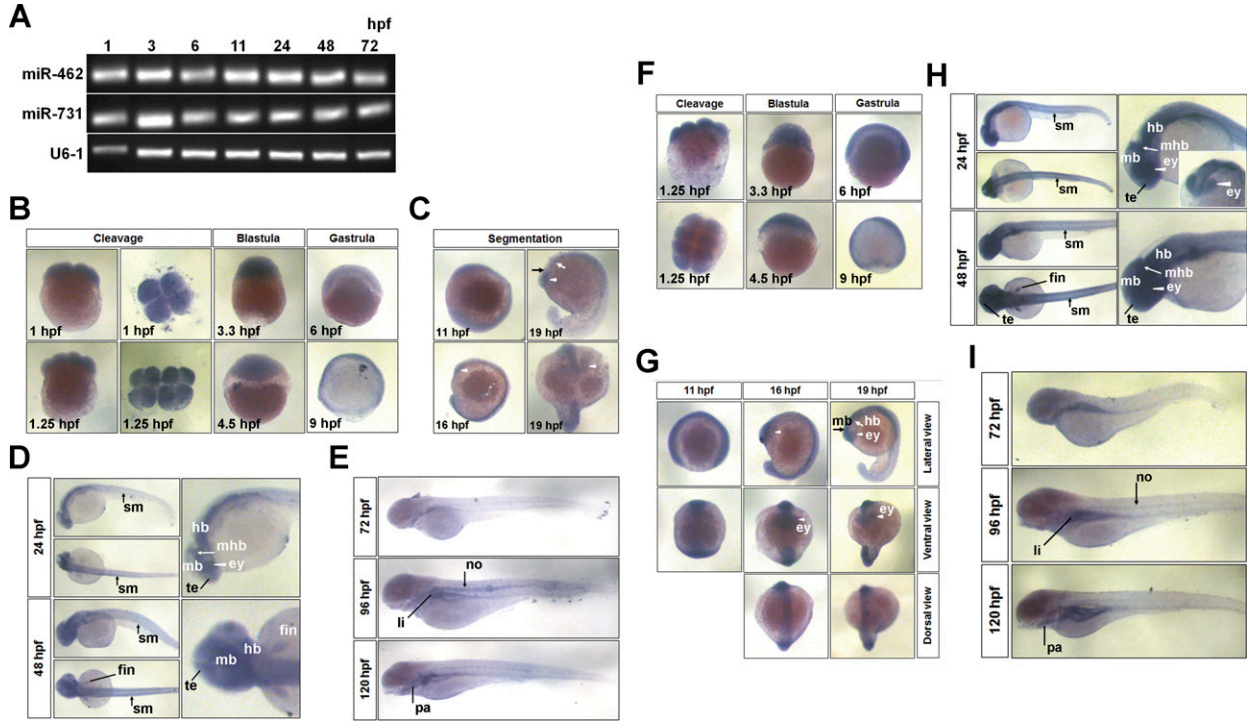

Figure 5. Spatiotemporal expression of miR-462/miR-731 cluster during zebrafish embryonic development. *A*) Temporal expression of miR-462 and miR-731 at indicated developmental stages detected by semiquantitative RT-PCR. U6-1 is used as endogenous control. *B–E*) Whole-mount *in situ* hybridization of miR-462 during embryogenesis in zebrafish. *B*) 1 hpf (4 cell), 1.25 hpf (8 cell), 3.3 hpf (high stage), 4.5 hpf (dome stage), 6 hpf (shield stage), and 9 hpf (90%–epiboly stage); *C*) segmentation period at 11, 16, and 19 hpf; *D*) 24 and 48 hpf, lateral and dorsal view; *E*) 72, 96, and 120 hpf, lateral view. ey, eye; mb, midbrain; hb, hind brain; mhb, midbrain–hind brain boundary; te, telencephalon; sm, somatic muscle; no, notochord; li, liver; pa, pharyngeal arch. *F–I*) Whole-mount *in situ* hybridization of miR-731 during embryogenesis in zebrafish. Expression pattern was detected at same developmental stages described above.

results indicated that Ddx5 is a *bona fide* target of miR-462 and can be effectively regulated under hypoxic stress.

miR-462 and miR-731 repress cell proliferation and induce apoptosis

Ddx5 and *ppm1da* are important elements involved in the p53 signaling pathway, which prompted interest in understanding whether the miR-462/miR-731 cluster contributes to cellular adaptation to hypoxic stress through crucial regulation pathways. Therefore, we investigated the involvement of miR-462 and miR-731 in cell survival.

We assessed the effect of miR-462 and miR-731 first on cell proliferation. As shown in **Fig. 4*A***, both miR-462 and miR-731 significantly suppressed the proliferation of ZF4 cells from 12 to 72 h, with no dose-dependent effect observed. Then we further analyzed their effect on cell cycle *via* flow cytometry analysis, and we found that the cells were efficiently synchronized at G2/M phase by treatment with nocodazole, while miR-462 and miR-731 significantly blocked the cell cycle progression of DNA replication at S phase, leading to the induction of the S-phase checkpoint (Fig. 4*B, C*). Meanwhile, we observed that the Cdk2 protein level was significantly increased along with the accumulation of G2/M cells but was reduced by the overexpression of miR-462 and miR-731 (Fig. 4*D*). This further confirmed that the cell cycle arrest is induced by miR-462 and miR-731. In addition, apoptosis assay revealed that overexpression of miR-462 and miR-731 resulted in a significant increase of the apoptosis level (Fig. 4*E*). Unexpectedly, no noticeable difference was detected in the corresponding caspase 3 activities (data not shown).

Temporospatial expression of miR-462/miR-731 cluster during zebrafish embryonic development

To examine the temporal expression pattern and anatomic localization of the zebrafish miR-462/miR-731

Figure 4. Both miR-462 and miR-731 repress cell proliferation through arresting cell cycle progress at S phase and induce cell apoptosis. *A*) ZF4 cells were transfected with miR-462 or miR-731 mimics (mock represents transfection control), and cell proliferation index was continuously detected using CCK-8 assay kit. All values represent means ± SE of triplicate determinations (**$P < 0.01$). *B*) Cell cycle phase analysis was performed by flow cytometry after synchronization with nocodazole. Untreated cells serve as control. Data correspond to means of 3 independent experiments. *C*) Percentage of cells in G1, S, and G2/M phase were determined. Results are presented as means ± SE ($n = 3$, *$P < 0.05$). +, cells treated with nocodazole for 12 h. *D*) Expression analysis of Cdk2 protein by Western blot analysis in corresponding ZF4 cell samples. β-Actin is used to normalize protein levels. *E*) ZF4 cells were transfected with miR-462 or miR-731 mimics, and percentage of apoptotic cells was determined by annexin V–FITC/propidium iodide staining and flow cytometry. Results are presented as means ± SE ($n = 3$, ***$P < 0.01$).

cluster during embryogenesis, the semi-qRT-PCR and whole-mount *in situ* hybridization were performed. qRT-PCR indicated that the miR-462/miR-731 cluster was continuously detectable from 1 h postfertilization (hpf) (cleavage stage) to 72 hpf (**Fig. 5*A***). The cluster was detected in a consistent and ubiquitous manner in the whole embryo throughout the early developmental stages up to 48 hpf (Fig. 5*B–D, F, G*). From 11 to 19 hpf, the cluster became enriched in the brain and the eye anlage (Fig. 5*C, G*). At 24 hpf, a weak expression was observed in somatic muscle, and stronger signals were detected in the eyes, telencephalon, midbrain, hind brain, and midbrain–hind brain boundary (Fig. 5*D, H*). At 48 hpf, a strong signal appeared in the fins (Fig. 5*D, H*). Later on, at 72 hpf, the signal became more prominent in the liver and gut regions (Fig. 5*E, I*). At 96 hpf and postfertiliztion d 5, the cluster was additionally detected in the pharyngeal arch region and the notochord, with strong signals remaining in liver (Fig. 5*E, I*). Overall, this genomic miRNA cluster, as expected, showed a similar expression pattern during zebrafish embryonic development.

DISCUSSION

Hypoxia occurs frequently in solid tumors because of an imbalance between the limited oxygen delivery capacity of the abnormal vasculature and the high oxygen consumption of tumor cells, which drives a complex and dynamic adaptive response to enable cells to survive this threat, including activation of several canonical signaling pathways. Recent evidence reveals that miRNA plays a crucial role among the complex and coordinated molecular mechanisms activated by hypoxia (18, 52). A subset of miRNAs, termed hypoxamirs, has recently been identified to be involved in a large number of cellular processes in response to low oxygen tension in mammal cells (52, 59, 60). Compared with mammals, fishes are noticeably more responsive to varying oxygen availability and have evolved a range of adaptive mechanisms to survive hypoxic stress (6), but our understanding is limited about the regulatory and physiologic functions of specific hypoxamirs in fishes. In the present study, we have identified a hypoxia-regulated miRNA cluster in zebrafish and uncovered its important role in regulating cell survival.

Among the 7 putative hypoxamirs identified in hypoxia exposed zebrafish by global expression profiling, the down-regulated miR-181a was previously reported to be hypoxia regulated in tumor conditions with contrasting changes in different tumor cells (61, 62), and the up-regulated miR-150 was inhibited in hypoxia-induced hepatocytes (63). Interestingly, miR-210, a demonstrated master hypoxamir across a wide range of mammalian cell types, was not significantly up-regulated (54); instead, we detected that a teleost-specific genomic miRNA cluster, miR-462/miR-731, was induced by hypoxic stress in both zebrafish larvae and ZF4 cells. These results imply the existence of a special hypoxamir community and regulatory system in fish. The target prediction analysis indicated that these putative hypoxamirs may be involved in important hypoxia-adaptive processes, including cell growth, glycolysis, and blood vessel morphogenesis. Recent evidence reveals that miR-451 regulates human erythropoiesis by targeting RAB14 (39), that miR-150 functions as a tumor suppressor in human colorectal cancer by targeting c-Myb (64), and that miR-181a regulates VEGF expression in chondrosarcoma cells. To date, in addition to zebrafish, the miR-462/miR-731 cluster has only been identified in medaka, channel catfish, and Atlantic salmon (miRBase), and little is known about its physiologic functions both at the embryonic and cellular levels.

It was reported that zebrafish miRNAs are extensively (~50%) encoded within polycistronic transcripts, including the miR-462/miR-731 cluster (65). As a genomic miRNA cluster residing within 200 bp, miR-462 and miR-731 may share common *cis*-regulatory elements, resulting in a coordinated expression pattern and combinatorial regulatory functions in response to hypoxia. Several hypoxia-responsive TFs play important regulatory roles under hypoxic cellular conditions (8). Among them, HIF-1, a master transcriptional regulator that mediates oxygen homeostasis, plays a predominant role in coordination of transcriptional changes under hypoxic stress, and direct HIF-1-driven regulation of hypoxamir transcription has been validated (18, 47). Here, we confirmed by promoter reporter assay that the miR-462/miR-731 cluster is a transcriptional target of Hif-1α. The cluster is significantly induced in accordance with Hif-1α under hypoxic conditions and the knockdown of Hif-1α by shRNA results in the inhibition of miR-462/miR-731 expression. These data suggest that Hif-1α contributes to the up-regulation of the hypoxia-induced miR-462/miR-731 cluster both in zebrafish embryos and ZF4 cells.

We observed that the endogenous Ddx5 protein level was significantly reduced along with the up-regulation of Hif-1α in ZF4 cells treated with $CoCl_2$ in a time-dependent manner, suggesting the oxygen-sensitive expression of Ddx5. It was previously reported that the DEAD box family is particularly sensitive to hypoxia, with at least 20 members significantly down-regulated, including DDX5 (p68) and DDX17 (p72) (66). DDX5 and DDX17 function as crucial coregulators of several TFs (including p53, NF-κB, and E2F1) and are involved in multiple cellular processes (67, 68). In addition, they control the biogenesis of miRNAs *via* their interaction with the Drosha/DGCR8 complex (69). Several lines of evidence demonstrate a DDX5/DDX17/miRNA feedback regulatory loop, in which DDX5 and DDX17 are recruited on the promoters along with key TFs and promote the expression of a specific miRNA, which in turn directly down-regulates the expression of DDX5 and DDX17 (67). Our results verified that the 3′ UTR of *ddx5* is a *bona fide* target of miR-462, and that miR-462 represses endogenous Ddx5 mRNA and protein expression. It is possible that Ddx5 may serve as a key transcriptional coregulator of HIF-1α in mediating induction of miR-462/miR-731 (or other hypoxamirs) under hypoxic stress, but further studies are needed to support this hypothesis. Additionally, DDX5 is required for DNA replication and cell proliferation, and the efficiency of DNA replication in S-phase cells is reduced upon DDX5 depletion (70). In the present study, the overexpression of miR-462 significantly enriched S-phase cells, indicating an increased duration of S phase, an induction of intra-S checkpoint, and significant repression of cell proliferation in a time-dependent manner. A reduction of Cdk2 protein was also detected, further confirming that miR-462 induces the cell cycle arrest.

Furthermore, miR-462 induces apoptosis, but probably not in a caspase 3–mediated manner. On the basis of all the aforementioned data, we hypothesize that miR-462 may influence cellular processes and regulate cell survival through the down-regulation of Ddx5. On the other hand, miR-731 was also observed to have a similar effect on cell growth and cell cycle progress. Although *ppm1da* was recognized as a downstream target of miR-731 and was annotated to p53 signaling pathway, it is currently uncertain whether *ppm1da* mediates the effect of miR-731 on cellular processes. However, as polycistronic transcripts, miR-462 and miR-731 may have a highly cooperative regulatory function in an intricate cellular signaling network. Further work is needed to decipher the combinatorial and hierarchical regulation mechanism by identifying overlapping downstream targets of miR-462 and miR-731. Additionally, it was reported that HIFs can change the miRNA signature of cells, which in turn can influence cell cycle progression, and hypoxia can block DNA replication in a HIF-1α–mediated manner (71). Therefore, we hypothesize that miR-462 and miR-731 may function in cellular adaptation to hypoxia *via* HIF-1α.

miRNAs have been established as key elements in zebrafish embryonic development (72, 73). The temporal expression and spatial distributions of multiple miRNAs have been demonstrated by microarrays and *in situ* hybridization during zebrafish development, but no signal was detected for miR-462 and miR-731 during early development stages (65, 74). Here, we observed that the zebrafish miR-462/miR-731 cluster was ubiquitously and consistently expressed in the whole embryo with no spatial restriction throughout the early developmental stages (1-cell stage to pectoral fin stage), which is in accordance with corresponding targets (*ddx5* and *ppm1da*) identified by Thisse *et al.* (unpublished data; *http://zfin.org*). It was revealed that late oogenesis and early embryogenesis rely exclusively on maternal mRNAs that subsequently undergo a general decay in embryos during the maternal-to-zygotic transition (75). Recent data in mice showed that gene regulation by miRNA is inactive before this transition (76, 77). However, miRNA has been identified as a major component of the zygotic mRNA decay pathway in both vertebrates and invertebrates. miRNA-dependent mRNA decay was first identified in zebrafish, with miR-430 expressed at the onset of zygotic transcription and the deadenylation and degradation of hundreds of maternal mRNAs facilitated during early embryogenesis (78). In the present study, strong signals of the miR-462/miR-731cluster were detected as early as at the cleavage stage, implying its potential role in maternal transcript clearance. Additionally, miR-462 was reported to be implicated in vitellogenesis of zebrafish (79). The miR-462/miR-731 cluster was continuously expressed, with enrichment occurring sequentially in the brain, eye, somatic muscle, and fins, suggesting its participation in organogenesis. Remarkably, the signal became more restricted to notochord, liver, and gut region from postfertilization d 3 to 5, which is similar to the expression pattern of zebrafish Hif-1α detected previously (27). Recent evidence shows that the miR-462/miR-731 cluster is also present in male liver of marine medaka (80). We therefore hypothesize that miR-462 and miR-731 may be essential for liver formation or growth, but further studies are needed to define their exact role. Overall, the data suggest the indispensable physiologic functions of the miR-462/miR-731 cluster during zebrafish embryonic development.

Taken together, the present study has confirmed miR-462/miR-731 as a teleost-specific miRNA cluster that is induced by hypoxia in a Hif-1α–mediated manner and has demonstrated its important role in regulating cell survival by targeting downstream genes. The overall results suggest that both miR-462 and miR-731 serve as important signaling intermediates in cellular adaptation to hypoxic stress. Furthermore, the expression profile indicates that the miR-462/miR-731 cluster is of physiologic significance and close relevance to organogenesis and embryonic development of zebrafish. Our findings provide some new insights into the role of hypoxamirs in cellular adaptation to hypoxia in zebrafish. FJ

This work was supported in part by the National Science Foundation of China (30901099), the Fundamental Research Funds for the Central Universities (2013PY067), Scientific Research Foundation for Returned Scholars, Ministry of Education of China, and Huazhong Agricultural University Scientific and Technological Self-Innovation Foundation (2013SC10).

REFERENCES

1. Schaffer, K., and Taylor, C. T. (2015) The impact of hypoxia on bacterial infection. *FEBS J.* **282**, 2260–2266 [E-pub ahead of print]
2. Nathaniel, T. I., Williams-Hernandez, A., Hunter, A. L., Liddy, C., Peffley, D. M., Umesiri, F. E., and Imeh-Nathaniel, A. (2015) Tissue hypoxia during ischemic stroke: adaptive clues from hypoxia-tolerant animal models. *Brain Res. Bull.* **114**, 1–12
3. Span, P. N., and Bussink, J. (2015) Biology of hypoxia. *Semin. Nucl. Med.* **45**, 101–109
4. Val, A. L., Gomes, K. R., and de Almeida-Val, V. M. (2015) Rapid regulation of blood parameters under acute hypoxia in the Amazonian fish *Prochilodus nigricans*. *Comp. Biochem. Physiol. A Mol. Integr. Physiol.* **184**, 125–131
5. Nathaniel, T. I., Soyinka, J. O., Adedeji, A., and Imeh-Nathaniel, A. (2015) Molecular and physiological factors of neuroprotection in hypoxia-tolerant models: pharmacological clues for the treatment of stroke. *J. Exp. Neurosci.* **9**, 1–5
6. Xiao, W. (2015) The hypoxia signaling pathway and hypoxic adaptation in fishes. *Sci. China Life Sci.* **58**, 148–155
7. Wouters, B. G., and Koritzinsky, M. (2008) Hypoxia signalling through mTOR and the unfolded protein response in cancer. *Nat. Rev. Cancer* **8**, 851–864
8. Cummins, E. P., and Taylor, C. T. (2005) Hypoxia-responsive transcription factors. *Pflugers Arch.* **450**, 363–371
9. Kaelin, W. G., Jr., and Ratcliffe, P. J. (2008) Oxygen sensing by metazoans: the central role of the HIF hydroxylase pathway. *Mol. Cell* **30**, 393–402
10. Lendahl, U., Lee, K. L., Yang, H., and Poellinger, L. (2009) Generating specificity and diversity in the transcriptional response to hypoxia. *Nat. Rev. Genet.* **10**, 821–832
11. Majmundar, A. J., Wong, W. J., and Simon, M. C. (2010) Hypoxia-inducible factors and the response to hypoxic stress. *Mol. Cell* **40**, 294–309
12. Gao, J. L., and Chen, Y. G. (2015) Natural compounds regulate glycolysis in hypoxic tumor microenvironment. *BioMed Res. Int.* **2015**, 354143
13. Courtnay, R., Ngo, D. C., Malik, N., Ververis, K., Tortorella, S. M., and Karagiannis, T. C. (2015) Cancer metabolism and the Warburg effect: the role of HIF-1 and PI3K. *Mol. Biol. Rep.* **42**, 841–851
14. Weidemann, A., and Johnson, R. S. (2008) Biology of HIF-1alpha. *Cell Death Differ.* **15**, 621–627
15. Wenger, R. H., Stiehl, D. P., and Camenisch, G. (2005) Integration of oxygen signaling at the consensus HRE. *Sci. STKE* **2005**, re12
16. Mole, D. R., Blancher, C., Copley, R. R., Pollard, P. J., Gleadle, J. M., Ragoussis, J., and Ratcliffe, P. J. (2009) Genome-wide association of

hypoxia-inducible factor (HIF)-1alpha and HIF-2alpha DNA binding with expression profiling of hypoxia-inducible transcripts. *J. Biol. Chem.* **284**, 16767–16775
17. Yun, Z., Maecker, H. L., Johnson, R. S., and Giaccia, A. J. (2002) Inhibition of PPAR gamma 2 gene expression by the HIF-1-regulated gene DEC1/Stra13: a mechanism for regulation of adipogenesis by hypoxia. *Dev. Cell* **2**, 331–341
18. Seok, J. K., Lee, S. H., Kim, M. J., and Lee, Y. M. (2014) MicroRNA-382 induced by HIF-1α is an angiogenic miR targeting the tumor suppressor phosphatase and tensin homolog. *Nucleic Acids Res.* **42**, 8062–8072
19. Morote-Garcia, J. C., Rosenberger, P., Kuhlicke, J., and Eltzschig, H. K. (2008) HIF-1-dependent repression of adenosine kinase attenuates hypoxia-induced vascular leak. *Blood* **111**, 5571–5580
20. Xi, H., Gao, Y. H., Han, D. Y., Li, Q. Y., Feng, L. J., Zhang, W., Ji, G., Xiao, J. C., Zhang, H. Z., and Wei, Q. (2014) Hypoxia inducible factor-1α suppresses peroxiredoxin 3 expression to promote proliferation of CCRCC cells. *FEBS Lett.* **588**, 3390–3394
21. Minton, D. R., Fu, L., Chen, Q., Robinson, B. D., Gross, S. S., Nanus, D. M., and Gudas, L. J. (2015) Analyses of the transcriptome and metabolome demonstrate that HIF1α mediates altered tumor metabolism in clear cell renal cell carcinoma. *PLoS One* **10**, e0120649
22. He, G., Jiang, Y., Zhang, B., and Wu, G. (2014) The effect of HIF-1α on glucose metabolism, growth and apoptosis of pancreatic cancerous cells. *Asia Pac. J. Clin. Nutr.* **23**, 174–180
23. Dunwoodie, S. L. (2009) The role of hypoxia in development of the mammalian embryo. *Dev. Cell* **17**, 755–773
24. Wang, Y., Wan, C., Deng, L., Liu, X., Cao, X., Gilbert, S. R., Bouxsein, M. L., Faugere, M. C., Guldberg, R. E., Gerstenfeld, L. C., Haase, V. H., Johnson, R. S., Schipani, E., and Clemens, T. L. (2007) The hypoxia-inducible factor alpha pathway couples angiogenesis to osteogenesis during skeletal development. *J. Clin. Invest.* **117**, 1616–1626
25. Tomlinson, R. E., and Silva, M. J. (2015) HIF-1α regulates bone formation after osteogenic mechanical loading. *Bone* **73**, 98–104
26. Imanirad, P., and Dzierzak, E. (2013) Hypoxia and HIFs in regulating the development of the hematopoietic system. *Blood Cells Mol. Dis.* **51**, 256–263
27. Lin, T. Y., Chou, C. F., Chung, H. Y., Chiang, C. Y., Li, C. H., Wu, J. L., Lin, H. J., Pai, T. W., Hu, C. H., and Tzou, W. S. (2014) Hypoxia-inducible factor 2 alpha is essential for hepatic outgrowth and functions via the regulation of leg1 transcription in the zebrafish embryo. *PLoS One* **9**, e101980
28. Palazon, A., Goldrath, A. W., Nizet, V., and Johnson, R. S. (2014) HIF transcription factors, inflammation, and immunity. *Immunity* **41**, 518–528
29. Kulshreshtha, R., Ferracin, M., Wojcik, S. E., Garzon, R., Alder, H., Agosto-Perez, F. J., Davuluri, R., Liu, C. G., Croce, C. M., Negrini, M., Calin, G. A., and Ivan, M. (2007) A microRNA signature of hypoxia. *Mol. Cell. Biol.* **27**, 1859–1867
30. Kulshreshtha, R., Davuluri, R. V., Calin, G. A., and Ivan, M. (2008) A microRNA component of the hypoxic response. *Cell Death Differ.* **15**, 667–671
31. Bartel, D. P. (2004) MicroRNAs: genomics, biogenesis, mechanism, and function. *Cell* **116**, 281–297
32. Jackson, R. J., and Standart, N. (2007) How do microRNAs regulate gene expression? *Sci. STKE* **2007**, re1
33. He, L., and Hannon, G. J. (2004) MicroRNAs: small RNAs with a big role in gene regulation. *Nat. Rev. Genet.* **5**, 522–531
34. Guo, H., Ingolia, N. T., Weissman, J. S., and Bartel, D. P. (2010) Mammalian microRNAs predominantly act to decrease target mRNA levels. *Nature* **466**, 835–840
35. Li, L. C., Okino, S. T., Zhao, H., Pookot, D., Place, R. F., Urakami, S., Enokida, H., and Dahiya, R. (2006) Small dsRNAs induce transcriptional activation in human cells. *Proc. Natl. Acad. Sci. USA* **103**, 17337–17342
36. Morris, K. V., Chan, S. W., Jacobsen, S. E., and Looney, D. J. (2004) Small interfering RNA–induced transcriptional gene silencing in human cells. *Science* **305**, 1289–1292
37. Sinha, M., Ghatak, S., Roy, S., and Sen, C. K. (2015) microRNA-200b as a switch for inducible adult angiogenesis. *Antioxid. Redox Signal.* **22**, 1257–1272
38. Su, Z., Si, W., Li, L., Zhou, B., Li, X., Xu, Y., Xu, C., Jia, H., and Wang, Q. K. (2014) MiR-144 regulates hematopoiesis and vascular development by targeting meis1 during zebrafish development. *Int. J. Biochem. Cell Biol.* **49**, 53–63
39. Kim, M., Tan, Y. S., Cheng, W. C., Kingsbury, T. J., Heimfeld, S., and Civin, C. I. (2015) MIR144 and MIR451 regulate human erythropoiesis via RAB14. *Br. J. Haematol.* **168**, 583–597
40. Lu, Y. F., Zhang, L., Waye, M. M., Fu, W. M., and Zhang, J. F. (2015) MiR-218 mediates tumorigenesis and metastasis: perspectives and implications. *Exp. Cell Res.* **334**, 173–182
41. Tang, H., Lee, M., Sharpe, O., Salamone, L., Noonan, E. J., Hoang, C. D., Levine, S., Robinson, W. H., and Shrager, J. B. (2012) Oxidative stress–responsive microRNA-320 regulates glycolysis in diverse biological systems. *FASEB J.* **26**, 4710–4721
42. Yuan, J., Xiao, G., Peng, G., Liu, D., Wang, Z., Liao, Y., Liu, Q., Wu, M., and Yuan, X. (2015) miRNA-125a-5p inhibits glioblastoma cell proliferation and promotes cell differentiation by targeting TAZ. *Biochem. Biophys. Res. Commun.* **457**, 171–176
43. Zhang, Z., Hong, Y., Xiang, D., Zhu, P., Wu, E., Li, W., Mosenson, J., and Wu, W. S. (2015) MicroRNA-302/367 cluster governs hESC self-renewal by dually regulating cell cycle and apoptosis pathways. *Stem Cell Rep.* **4**, 645–657
44. Hatano, K., Kumar, B., Zhang, Y., Coulter, J. B., Hedayati, M., Mears, B., Ni, X., Kudrolli, T. A., Chowdhury, W. H., Rodriguez, R., DeWeese, T. L., and Lupold, S. E. (2015) A functional screen identifies miRNAs that inhibit DNA repair and sensitize prostate cancer cells to ionizing radiation. *Nucleic Acids Res.* **43**, 4075–4086
45. Xu, J., and Wong, C. (2008) A computational screen for mouse signaling pathways targeted by microRNA clusters. *RNA* **14**, 1276–1283
46. Piriyapongsa, J., Jordan, I. K., Conley, A. B., Ronan, T., and Smalheiser, N. R. (2011) Transcription factor binding sites are highly enriched within microRNA precursor sequences. *Biol. Direct* **6**, 61
47. Shan, F., Li, J., and Huang, Q. Y. (2014) HIF-1 alpha–induced up-regulation of miR-9 contributes to phenotypic modulation in pulmonary artery smooth muscle cells during hypoxia. *J. Cell. Physiol.* **229**, 1511–1520
48. Howell, J. C., Chun, E., Farrell, A. N., Hur, E. Y., Caroti, C. M., Iuvone, P. M., and Haque, R. (2013) Global microRNA expression profiling: curcumin (diferuloylmethane) alters oxidative stress–responsive microRNAs in human ARPE-19 cells. *Mol. Vis.* **19**, 544–560
49. Ishikawa, K., Ishikawa, A., Shoji, Y., and Imai, T. (2014) A genotoxic stress-responsive miRNA, miR-574-3p, delays cell growth by suppressing the enhancer of rudimentary homolog gene in vitro. *Int. J. Mol. Sci.* **15**, 2971–2990
50. Liu, F., Wang, W., Sun, X., Liang, Z., and Wang, F. (2015) Conserved and novel heat stress-responsive microRNAs were identified by deep sequencing in *Saccharina japonica* (Laminariales, Phaeophyta). *Plant Cell Environ.* **38**, 1357–1367
51. Nallamshetty, S., Chan, S. Y., and Loscalzo, J. (2013) Hypoxia: a master regulator of microRNA biogenesis and activity. *Free Radic. Biol. Med.* **64**, 20–30
52. Greco, S., and Martelli, F. (2014) MicroRNAs in hypoxia response. *Antioxid. Redox Signal.* **21**, 1164–1166
53. Kelly, T. J., Souza, A. L., Clish, C. B., and Puigserver, P. (2011) A hypoxia-induced positive feedback loop promotes hypoxia-inducible factor 1alpha stability through miR-210 suppression of glycerol-3-phosphate dehydrogenase 1-like. *Mol. Cell. Biol.* **31**, 2696–2706
54. Chan, Y. C., Banerjee, J., Choi, S. Y., and Sen, C. K. (2012) miR-210: the master hypoxamir. *Microcirculation* **19**, 215–223
55. Chan, S. Y., and Loscalzo, J. (2010) MicroRNA-210: a unique and pleiotropic hypoxamir. *Cell Cycle* **9**, 1072–1083
56. Chen, C., Ridzon, D. A., Broomer, A. J., Zhou, Z., Lee, D. H., Nguyen, J. T., Barbisin, M., Xu, N. L., Mahuvakar, V. R., Andersen, M. R., Lao, K. Q., Livak, K. J., and Guegler, K. J. (2005) Real-time quantification of microRNAs by stem-loop RT-PCR. *Nucleic Acids Res.* **33**, e179
57. Wienholds, E., Kloosterman, W. P., Miska, E., Alvarez-Saavedra, E., Berezikov, E., de Bruijn, E., Horvitz, H. R., Kauppinen, S., and Plasterk, R. H. (2005) MicroRNA expression in zebrafish embryonic development. *Science* **309**, 310–311
58. Kloosterman, W. P., Wienholds, E., de Bruijn, E., Kauppinen, S., and Plasterk, R. H. (2006) *In situ* detection of miRNAs in animal embryos using LNA-modified oligonucleotide probes. *Nat. Methods* **3**, 27–29
59. Brock, M., Haider, T. J., Vogel, J., Gassmann, M., Speich, R., Trenkmann, M., Ulrich, S., Kohler, M., and Huber, L. C. (2015) The hypoxia-induced microRNA-130a controls pulmonary smooth muscle cell proliferation by directly targeting CDKN1A. *Int. J. Biochem. Cell Biol.* **61**, 129–137
60. Rebucci, M., Sermeus, A., Leonard, E., Delaive, E., Dieu, M., Fransolet, M., Arnould, T., and Michiels, C. (2015) miRNA-196b

inhibits cell proliferation and induces apoptosis in HepG2 cells by targeting IGF2BP1. *Mol. Cancer* **14**, 79
61. Sun, X., Wei, L., Chen, Q., and Terek, R. M. (2015) MicroRNA regulates vascular endothelial growth factor expression in chondrosarcoma cells. *Clin. Orthop. Relat. Res.* **473**, 907–913
62. Agrawal, R., Pandey, P., Jha, P., Dwivedi, V., Sarkar, C., and Kulshreshtha, R. (2014) Hypoxic signature of microRNAs in glioblastoma: insights from small RNA deep sequencing. *BMC Genomics* **15**, 686
63. Yu, Z. Y., Bai, Y. N., Luo, L. X., Wu, H., and Zeng, Y. (2013) Expression of microRNA-150 targeting vascular endothelial growth factor-A is downregulated under hypoxia during liver regeneration. *Mol. Med. Rep.* **8**, 287–293
64. Feng, J., Yang, Y., Zhang, P., Wang, F., Ma, Y., Qin, H., and Wang, Y. (2014) miR-150 functions as a tumour suppressor in human colorectal cancer by targeting c-Myb. *J. Cell. Mol. Med.* **18**, 2125–2134
65. Thatcher, E. J., Bond, J., Paydar, I., and Patton, J. G. (2008) Genomic organization of zebrafish microRNAs. *BMC Genomics* **9**, 253
66. Guimbellot, J. S., Erickson, S. W., Mehta, T., Wen, H., Page, G. P., Sorscher, E. J., and Hong, J. S. (2009) Correlation of microRNA levels during hypoxia with predicted target mRNAs through genome-wide microarray analysis. *BMC Med. Genomics* **2**, 15
67. Dardenne, E., Polay Espinoza, M., Fattet, L., Germann, S., Lambert, M. P., Neil, H., Zonta, E., Mortada, H., Gratadou, L., Deygas, M., Chakrama, F. Z., Samaan, S., Desmet, F. O., Tranchevent, L. C., Dutertre, M., Rimokh, R., Bourgeois, C. F., and Auboeuf, D. (2014) RNA helicases DDX5 and DDX17 dynamically orchestrate transcription, miRNA, and splicing programs in cell differentiation. *Cell Reports* **7**, 1900–1913
68. Fuller-Pace, F. V. (2013) The DEAD box proteins DDX5 (p68) and DDX17 (p72): multi-tasking transcriptional regulators. *Biochim. Biophys. Acta* **1829**, 756–763
69. Suzuki, H. I., Yamagata, K., Sugimoto, K., Iwamoto, T., Kato, S., and Miyazono, K. (2009) Modulation of microRNA processing by p53. *Nature* **460**, 529–533
70. Mazurek, A., Luo, W., Krasnitz, A., Hicks, J., Powers, R. S., and Stillman, B. (2012) DDX5 regulates DNA replication and is required for cell proliferation in a subset of breast cancer cells. *Cancer Discov.* **2**, 812–825
71. Ortmann, B., Druker, J., and Rocha, S. (2014) Cell cycle progression in response to oxygen levels. *Cell. Mol. Life Sci.* **71**, 3569–3582
72. Ouchi, Y., Yamamoto, J., and Iwamoto, T. (2014) The heterochronic genes lin-28a and lin-28b play an essential and evolutionarily conserved role in early zebrafish development. *PLoS One* **9**, e88086
73. Tal, T. L., Franzosa, J. A., Tilton, S. C., Philbrick, K. A., Iwaniec, U. T., Turner, R. T., Waters, K. M., and Tanguay, R. L. (2012) MicroRNAs control neurobehavioral development and function in zebrafish. *FASEB J.* **26**, 1452–1461
74. Kloosterman, W. P., Steiner, F. A., Berezikov, E., de Bruijn, E., van de Belt, J., Verheul, M., Cuppen, E., and Plasterk, R. H. (2006) Cloning and expression of new microRNAs from zebrafish. *Nucleic Acids Res.* **34**, 2558–2569
75. Barckmann, B., and Simonelig, M. (2013) Control of maternal mRNA stability in germ cells and early embryos. *Biochim. Biophys. Acta* **1829**, 714–724
76. Svoboda, P. (2010) Why mouse oocytes and early embryos ignore miRNAs? *RNA Biol.* **7**, 559–563
77. Suh, N., Baehner, L., Moltzahn, F., Melton, C., Shenoy, A., Chen, J., and Blelloch, R. (2010) MicroRNA function is globally suppressed in mouse oocytes and early embryos. *Curr. Biol.* **20**, 271–277
78. Giraldez, A. J., Mishima, Y., Rihel, J., Grocock, R. J., Van Dongen, S., Inoue, K., Enright, A. J., and Schier, A. F. (2006) Zebrafish MiR-430 promotes deadenylation and clearance of maternal mRNAs. *Science* **312**, 75–79
79. Cohen, A., and Smith, Y. (2014) Estrogen regulation of microRNAs, target genes, and microRNA expression associated with vitellogenesis in the zebrafish. *Zebrafish* **11**, 462–478
80. Lau, K., Lai, K. P., Bao, J. Y., Zhang, N., Tse, A., Tong, A., Li, J. W., Lok, S., Kong, R. Y., Lui, W. Y., Wong, A., and Wu, R. S. (2014) Identification and expression profiling of microRNAs in the brain, liver and gonads of marine medaka (*Oryzias melastigma*) and in response to hypoxia. *PLoS One* **9**, e110698

Received for publication November 3, 2014.
Accepted for publication August 3, 2015.